ISSN: 2414-1895 DOI: 10.6919/ICJE.202512_11(12).0014

The Influence of Negative Stress on the Electronic Structure and Optical Properties of SnS_2

Longqin Wu

Department of basic education, Qiannan preschool education college for nationalities, Guiding, Qiandongnan Miao and Dong Autonomous Prefecture 558200, China

Abstract

With the rapid development of today's society, traditional materials no longer meet the development needs of China's optoelectronic and semiconductor materials. This article fully analyzes the optoelectronic properties of SnS_2 under negative stress through first principles and molecular dynamics theory, and deeply explores the influence of SnS_2 of optical properties under negative stress. The paper adopts first principles as the main research method to investigate the changes and effects of electronic structure and optical properties of SnS_2 before and after applying negative stress. Research has shown that negative stress has a significant improvement effect on the optical properties of SnS_2. Under negative stress, the band gap of the band structure generally decreases, and there is no band gap at -25 GPa; The total density of states and partial density of states decrease with the decrease of stress, and the electron density and maximum peak also decrease, but both are higher than those at 0 GPa; The reflectivity fluctuates and decreases with the decrease of stress; The absorption rate only increases at -10 GPa and shows a decreasing trend under other stresses; The refractive index shows a trend of first decreasing and then increasing, reaching a maximum value of 6.11 under the stress of -25 GPa; The ability loss function fluctuates and increases with the change of stress, with a maximum energy loss of 11.92 at -10 GPa.

Keywords

SnS_2; Stress; Electronic Structure; Optical Properties; First Principle.

1. Introduction

SnS_2 is an emerging two-dimensional material that has received extensive attention and research in multiple fields in recent years due to its excellent performance in various properties [1-3]. SnS_2 is usually a golden yellow sheet-like crystal with a layered structure and symmetry, and has good stability. SnS_2 has certain reflection and absorption characteristics for light, and also exhibits some semiconductor characteristics. In long-term research, it has been found that SnS_2 is an n-type semiconductor material with a bandgap width of about 2.0~2.4 eV. When adjusted to a certain bandgap width, SnS_2 exhibits good optical and electrical properties, and can be widely used in optoelectronic and semiconductor materials [4].

SnS_2 as an *n*-type semiconductor material, has excellent gas sensing performance and can detect low concentrations of toxic and harmful gases such as NH_3 and H_2S. Due to its low cost, environmental friendliness, and abundant global reserves, SnS_2 has broad application prospects in the field of gas detection[5-8]. With the development of technology, the gas sensing performance of SnS_2 has been significantly improved through surface treatment and micro control, providing new ideas for the development of gas sensors. The layered structure of SnS_2 allows it to provide specific channels and interfaces, facilitating the separation and transport of photogenerated charges. The layered structure also enhances light absorption capacity, provides more reactive sites, thereby improving light

ISSN: 2414-1895 DOI: 10.6919/ICJE.202512_11(12).0014

utilization and photocatalytic efficiency [6-9]. Therefore, SnS_2 has significant advantages in photoelectric conversion and photocatalytic applications.

In recent years, due to the outstanding performance of metal sulfide semiconductor materials in the fields of optics, electrical energy storage, and photoelectric conversion, they have received increasing attention from experts and scholars. SnS_2 has a simple and non-toxic elemental composition, diverse structures, and has gradually become a research hotspot in the fields of optics and semiconductors. Domestic and foreign scholars have been continuously researching SnS_2 materials in the field of photocatalysis, especially in environmental remediation and energy conversion [10-13]. Through repeated experiments and extensive calculations, they are constantly seeking ways to optimize the photocatalytic mechanism and performance of SnS_2 materials. In early research, it was found that the electrochemical performance of SnS_2 was not very ideal. However, with the development and application of science and technology, SnS_2 materials have been processed through advanced equipment and methods, and their electrochemical performance has been greatly improved.

In their research, Rao Yu et al. found that SnS_2 has a very high-volume expansion rate during hydrogen storage, which greatly reduces the service life and energy storage capacity of the battery [14]. In order to alleviate the volume expansion of metal sulfides during charging and discharging, it is necessary to optimize its structural design, introduce higher precision machinery for processing, and use carbon materials with higher mechanical strength to solve the problem of volume expansion of metal sulfides during charging and discharging.

Graphene is a typical two-dimensional carbon nanomaterial, which was discovered by Geim and Novoselov in 2004 and won the Nobel Prize in Physics in 2010. Since its discovery, graphene has been widely used in various battery applications and research and development [15]. Hao Wen, Zhou Peng, and others from Sichuan University used graphene powder (GP) to composite with SnS_2, and then analyzed and compared its charge and discharge capacity with pure SnS_2[16]. The first discharge capacity of pure SnS_2 was 1171.5 mAh/g, the charge capacity was only 371.19 mAh/g, and the first coulombic efficiency was only 31%. Compared with the composite SnS_2/GP sample, the first discharge capacity and charge capacity of the composite sample reached 1525.34 and 582.7 mAh/g, respectively, and the first coulombic efficiency (CE) increased from 31% to 38%[17]. After two cycles, the discharge and charge capacities of pure SnS_2 and SnS_2/GP samples decreased to 340.9 mAh/g, 330.3 mAh/g, 619.9 mAh/g, and 579.4 mAh/g, respectively. Compared with pure SnS_2, the composite SnS_2/GP material has a higher capacity [18].

In 2013, Xiang Hua Hu et al. published an article on the preparation of SnS, SnS_2, and SnS/SnS_2 heterojunction materials using a one-step pyrolysis method [19]. The study found that the prepared materials have excellent photoresponsivity properties, and compared with pure SnS and SnS_2, SnS/SnS_2 heterojunction materials have a certain improvement in photocatalytic performance for the photodegradation of organic dyes [20]. Huang Guozhou found that using SnS_2 nanosheets as the substrate, MoS_2 nanosheets were combined with them through hydrothermal synthesis to form a MoS_2/In_2S_3 two-dimensional/two-dimensional heterojunction [21]. At the optimal composite ratio, the photocatalytic performance of this heterojunction was improved by 81% compared to pure SnS_2 [22]. This is because the heterojunction is formed in a face-to-face contact manner, which increases the carrier mobility. In 2019, Yong Jiang's team synthesized SnS_2/graphene/SnS_2 (SnS_2/rGO/SnS_2) composite materials using a simple one-step hydrothermal method [23]. Through their research, the team found that the interlayer spacing of SnS_2 in the composite material increased to -8.03 Å compared to the original, which was beneficial for the insertion/extraction of Li^+ and Na^+, and inhibited the re stacking of SnS_2 nanosheets during charge and discharge cycles. After 200 cycles, SnS_2 nanoparticles did not undergo significant morphological changes and could still recover to their original phase without obvious agglomeration. Studies have shown that the composite material has high-rate performance and high cycling stability, making it a lithium/sodium battery [24]. Excellent materials for electrode production.

ISSN: 2414-1895 DOI: 10.6919/ICJE.202512_11(12).0014

This article adopts first principles and molecular dynamics research methods, uses MS software for simulation calculations, constructs a structural model of SnS_2, and compares the unstressed and negatively stressed SnS_2 by applying negative stress to explore the influence of negative stress on the electronic structure and optical properties of SnS_2. Analyze the performance changes of SnS_2 under different negative stresses, explore its applicable fields and future development directions.

2. Calculation Methods and Models

SnS_2 belongs to the hexagonal crystal system, with a space group and lattice constant of 186; A=b=3.68 Å, c=12.34 Å, α=β=90°, γ=120° [25]. The internal coordinates are S (0,0,0.0065), Sn (0.333, 0.667, 0.625), Sn (0.667, 0.333, 0.7434), and the atomic structure model is shown in Figure 1. Negative stress is used to regulate the electronic structure and optical properties of SnS_2. The direction of negative stress regulation is in the [110] direction, and the selection range of stress magnitude is -5 GPa~-25 GPa, decreasing at intervals of -5 GPa.

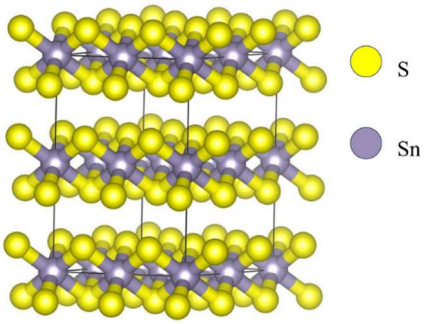

Figure 1. The atomic structural model of SnS_2

All the calculation work was completed by the CASTEP (Cambridge sequential total energy package) software package, and the BFGS algorithm was used to finely optimize the geometric structure of the system, obtaining a stable system structure. The electronic structure and optical properties of SnS_2 were calculated based on this. The calculated test parameters are as follows: using Ultra soft pseudo potential USPP (Ultra soft pseudo potential) to process the interaction between ions and electrons, and using generalized gradient approximation GGA (The generalized gradient approximation), PBE (Perdew Becke Ernerhof) exchange correlation functional to process and calculate the exchange correlation energy between electrons. Set the cutoff energy to 420 eV, the convergence threshold for interatomic forces to be 0.05 eV/nm, the internal stress to be less than 0.1 GPa, and the convergence threshold for atomic displacement to be 0.02 pm. The energy convergence standard between the two iterations is set to 2.0 × 10-5 eV/atom. The K point in the Monkors Pack Brillouin zone is selected as 4 × 5 × 3, and the valence state electrons involved in the calculation are selected Sn: $4d^{10}5d^{2}5p^{2}$, S: $3s^{2}3p^{4}$.

3. Results and Discussion

3.1 Electronic Structure

To understand the conductivity and optical properties of a material, it is necessary to know its bandgap width. The bandgap width range of 3-0 eV is generally for semiconductors, while conductors do not have a bandgap width. If it is greater than 3 eV, it is considered an insulator. Figure 2 (a) shows the band structure of SnS_2 at 0 GPa. The Fermi level is located at the zero mark on the y-axis, with the conduction band and valence band above and below the Fermi level. The difference between the two is called the bandgap, also known as the band gap. From Figure 2 (a), it can be seen that the bottom of the conduction band is at M~L in the Brillouin zone, with a minimum value of 1.47 eV, and the

ISSN: 2414-1895 DOI: 10.6919/ICJE.202512_11(12).0014

top of the valence band is at G, with a maximum value of 0 eV and a bandgap of 1.47 eV. Therefore, it can be concluded that SnS2 exhibits the properties of an indirect bandgap semiconductor at 0 GPa.

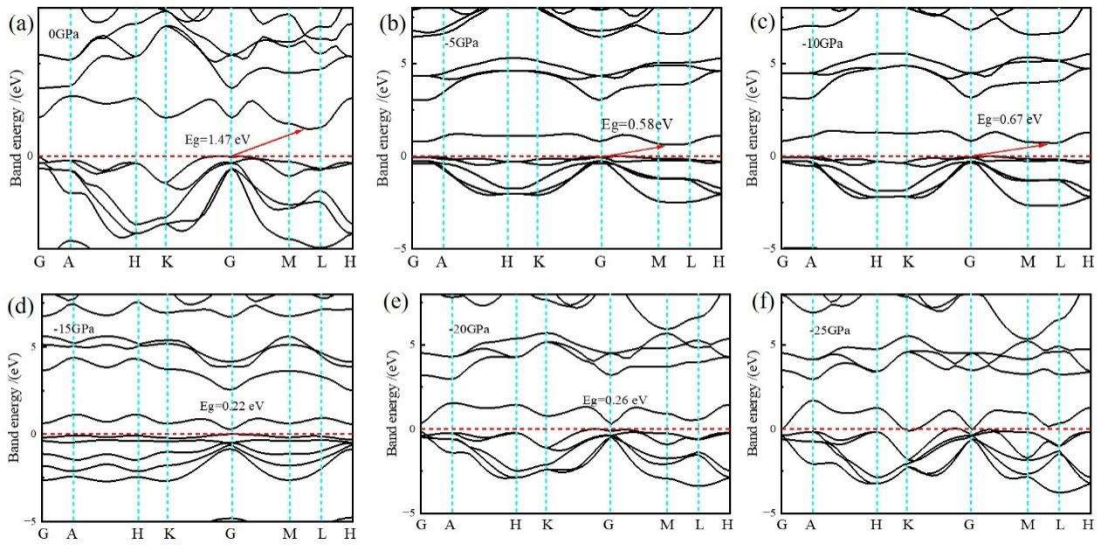

Figure 2. Band structure of SnS_2 under different negative stresses (a) 0 GPa, (b)-5 GPa, (c)-10 GPa, (d)-15 GPa, (e)-20 GPa, (f)-25 GPa

Under the influence of different negative stresses, the band structure of SnS_2 undergoes corresponding changes, with changes in the position distribution of the conduction band bottom and valence band top, as well as changes in the bandgap width. The specific situation is shown in the figure and the following analysis. From Figure 2 (b) - (f), it can be seen that under a stress of -5 GPa, the bottom of the conduction band is in the M~L region, and the top of the valence band is at the G point. The minimum value of the bottom of the conduction band is 0.58 eV, so the bandgap value under this stress is 0.58 eV. Under a stress of -10 GPa, the positions of the bottom and top of the conduction band are not significantly different from those under -5 GPa, except for a slight widening of the bandgap, which is 0.67 eV. At -15 GPa, compared with the front, the positions of the bottom and top of the valence band are both at the G point, and the lowest point of the conduction band is 0.22 eV, so the bandgap value at this time is 0.22 eV. At -20 GPa, although the stress decreases, there is little change compared to -15 GPa. The positions of the conduction band bottom and valence band top are still at the G point, but the bandgap slightly widens from 0.22 eV to 0.26 eV. At -25 GPa. The band structure of SnS_2 undergoes the greatest change, with the conduction band and valence band overlapping each other and no bandgap. The bottom of the conduction band and the top of the valence band are located at different positions in the K~G region. Under the action of negative stress, compared with the case without stress, the band gap of SnS_2 decreases overall with the decrease of stress. The decrease in band gap width indicates that valence electrons are more likely to transition to the conduction band, thereby increasing the number of free electrons and holes and improving conductivity. A smaller band gap width indicates that the material has strong absorption ability for visible light. So SnS_2 has good optoelectronic properties, especially at -25 GPa, where there is no bandgap, indicating that SnS_2 has the best optoelectronic performance compared to other stresses in this situation.

ISSN: 2414-1895 DOI: 10.6919/ICJE.202512_11(12).0014

3.2 Electronic Density of States

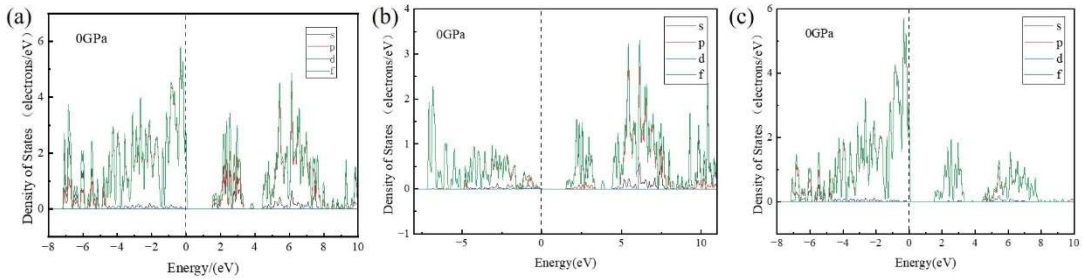

Figure 3. Density of Electronic States at 0GPa (a) SnS_2, (b) Sn, (c)S

Figure 3 (a) shows the total electron density of states of SnS_2 at 0 GPa. From the graph, it can be seen that between -7 eV and -4.68 eV, the contribution to the density of states is mainly made by s, p, and d state electrons. In this range, the contribution of p state electrons is slightly smaller than that of s state electrons. In the energy range of -4.68~0 eV, the contribution of s-state electrons is relatively small compared to p-state electrons, and the density of states is mainly contributed by p-state electrons. Between 0 and 10 eV, the contribution of p-state electrons is relatively large, while the contribution of other state electrons is relatively small; Figure 3 (b) shows the density of states of Sn electrons at 0 GPa. It can be seen from the figure that in the energy range of -7 to 0 eV, the contribution is mainly made by p and d state electrons, while the contribution of s and d state electrons is very small. In the range of 0 to 10 eV, the contribution of s state electrons is much greater than that of the previous region, but it is still relatively small compared to the contribution of p state electrons. Figure 3 (c) shows the density of states of S electrons at 0 GPa. It can be seen from the graph that S state electrons only make a slight contribution at the beginning of the energy increase, and their contribution to the overall effect is negligible. The main contribution is still from p and d state electrons.

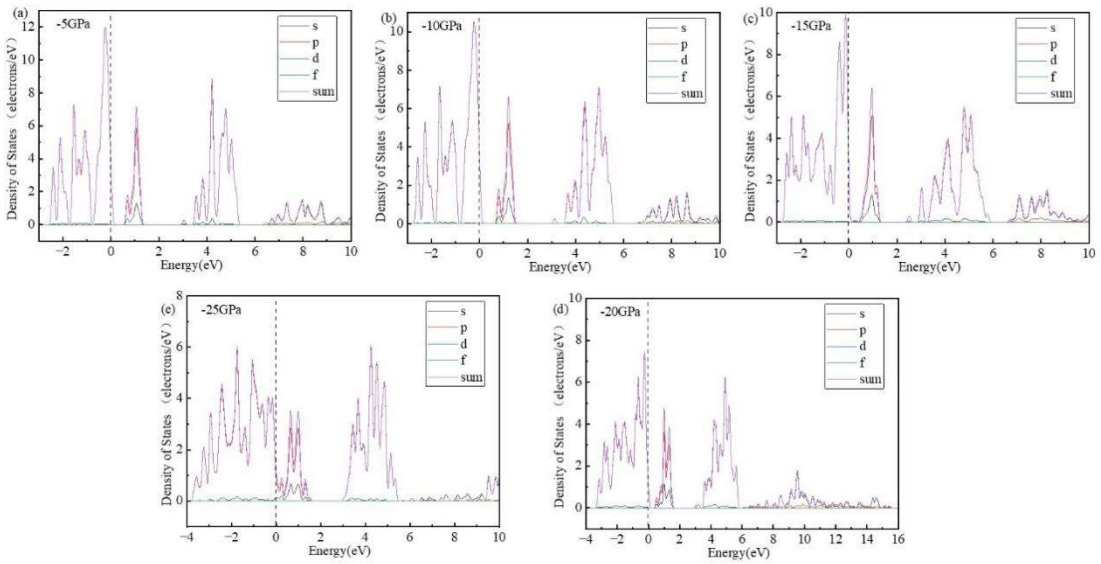

Figure 4. Electronic density of states of SnS_2 under different negative stresses a)-5 GPa, b)-10 GPa, c)-15 GPa, d)-20 GPa, e)-25 GPa

Figure 4 shows the total electron density of states of SnS_2 under different negative stresses. It can be seen from the figure that under these five negative stresses, both the conduction and valence bands are mainly contributed by p-state electrons, while the contribution of other state electrons is very small; The main changes are peak and electron density. As the stress decreases, the electron density and maximum peak also decrease, but both are larger than those at 0 GPa. As shown in Figure 5, the

ISSN: 2414-1895 DOI: 10.6919/ICJE.202512_11(12).0014

electronic density of states of Sn under different negative stresses. Under five negative stresses of -5 GPa, -10 GPa, -15 GPa, -20 GPa, and -25 GPa, the electron density of Sn is roughly the same, with changes in the maximum peak and electron density. Both the valence and conduction bands are mainly contributed by p-state electrons, with very little contribution from other state electrons. From the graph, it can be seen that the decrease in stress leads to a decrease in both electron density and maximum peak value. Compared to 0 GPa, both electron density and maximum peak value increase, and are higher than those at 0 GPa.

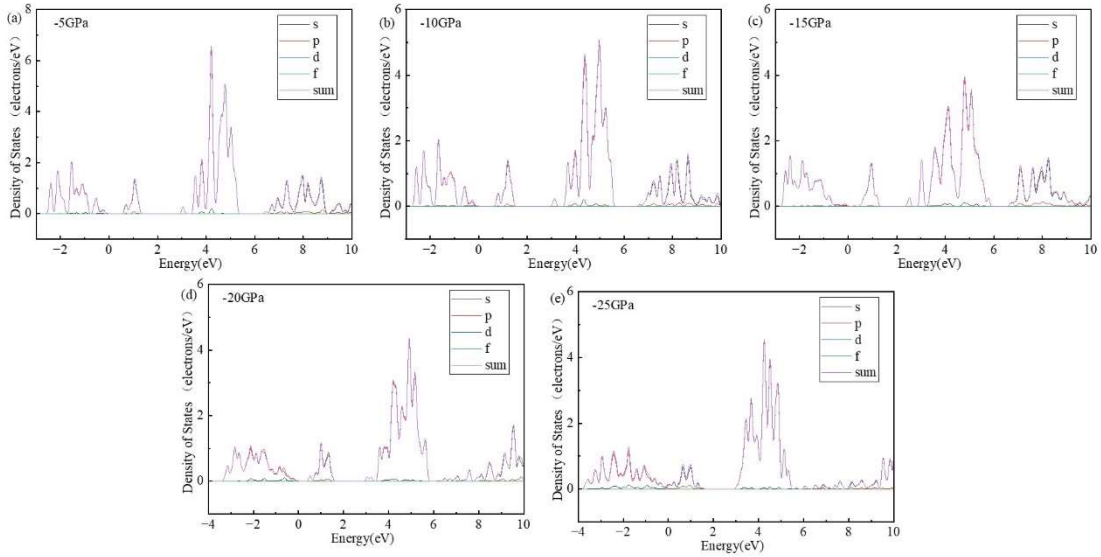

Figure 5. Electronic density of states of Sn under different negative stresses a)-5 GPa, b)-10 GPa, c)-15 GPa, d)-20 GPa, e)-25 GPa

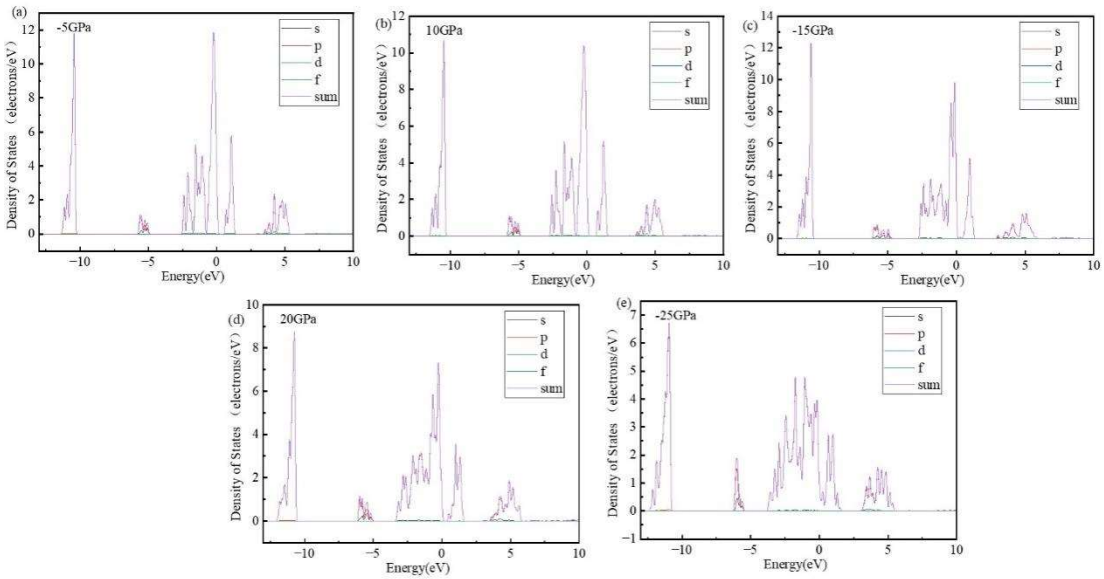

Figure 6. Electronic density of states of S under different negative stresses a)-5 GPa, b)-10 GPa, c)-15 GPa, d)-20 GPa, e)-25 Gpa

From Figure 6, it can be seen that the overall difference in the electronic density of states of S under different stresses is not significant, with the main differences being the maximum peak and electron density. -12.43-10.67 eV is mainly contributed by s-state electrons, but this region is far away from the optical bandgap and relatively isolated, with almost no effect on the Fermi level and optical

ISSN: 2414-1895 DOI: 10.6919/ICJE.202512_11(12).0014

properties. Other regions are mainly contributed by p-state electrons, and the contribution of other state electrons is negligible or even zero. From the overall trend of the graph, it can be seen that as the stress decreases, the maximum peak value and electron density also decrease. Compared with 0 GPa, only -25 GPa is lower than 0 GPa, while the rest are higher than 0 GPa.

3.3 Optical Properties

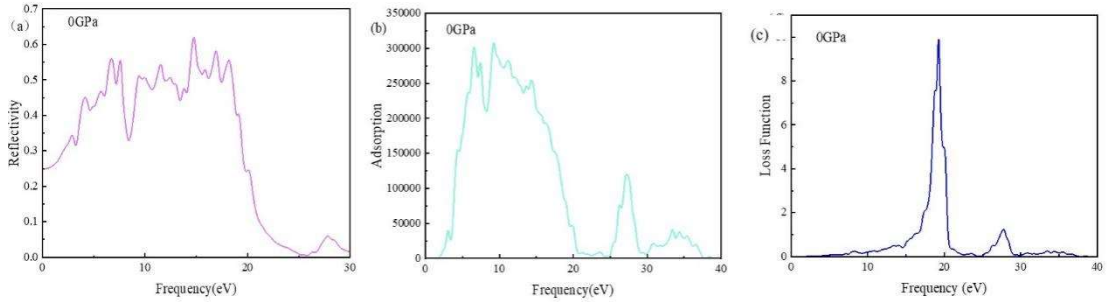

Figure 7. the optical properties of SnS_2 at 0 GPa: a) Reflectance, b) Absorption, c) Loss Function

Figure 7 (a) shows the reflectance of SnS_2 at 0 GPa. Reflection phenomenon begins to occur when the energy increases to 0.01 eV, with an initial reflectivity of 0.244. When the energy increases to the range of 2.7-14.73 eV, the reflectivity shows a fluctuating growth trend. At an energy of 14.73 eV, the reflectivity reaches a maximum peak of 0.62. After 14.73 eV, the reflectivity sharply decreases with the increase of energy, although there is a slight fluctuation, the impact is small, and it eventually approaches zero. Figure 7 (b) shows the absorption rate of SnS_2 at 0 GPa. The absorption phenomenon begins with an increase in energy. When the energy reaches 1.7 eV, the absorption rate suddenly increases and shows an overall upward trend. The first peak appears at 6.5 eV, and the second peak appears as the energy increases to 9.2 eV. This is also the maximum value of SnS_2 absorption rate at 0 GPa, which is 3.08964×10^5 cm^{-1}. As the energy continues to increase to 24.2 eV, the reflectivity gradually decreases and approaches zero. When the energy continues to increase to 27.3 eV, a third peak appears, but it is smaller compared to the previous two peaks, and the electron transition ability is relatively weak. Figure 7 (c) shows the energy loss function of SnS2 at 0 GPa. From the graph, it can be seen that the energy loss is relatively small before 14.66 eV. As the energy continues to increase, the maximum peak energy loss of 9.93 appears at 19.2 eV. As the energy continues to increase, the energy loss sharply decreases. After 20.84 eV, the dielectric function graph becomes flat and the energy loss gradually decreases.

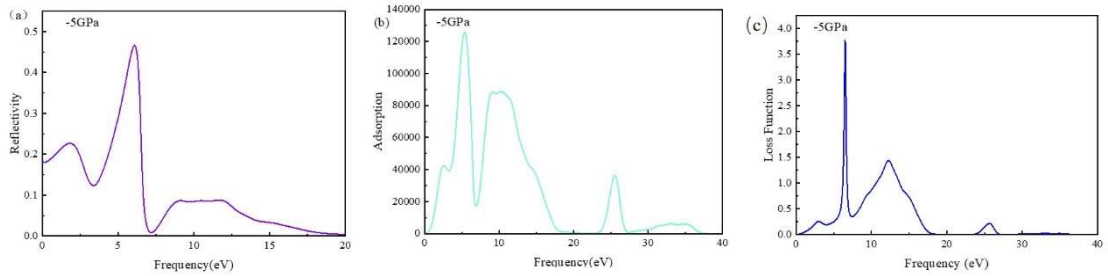

Figure 8. the optical properties of SnS_2 at -5 GPa: a) Reflectance, b) Absorption, c) Loss Function

Figure 8 (a) shows the reflectance of SnS_2 at -5 GPa. As shown in the figure, within the energy range of 0-7.17 eV, the reflectivity increases as the energy increases. However, there is a reverse increase between 1.83-3.37 eV, and then it continues to increase until reaching a maximum peak of 0.46 at 7.17 eV. As the energy continues to increase, the reflectivity decreases overall and eventually approaches zero. Figure 8 (b) shows the absorption rate of SnS_2 at -5 GPa. As the energy begins to increase, the absorption coefficient increases and reaches its maximum peak at 1.26174×10^5 cm^{-1} at

ISSN: 2414-1895 DOI: 10.6919/ICJE.202512_11(12).0014

5.36 eV. It then sharply decreases to 1.6397 × 104 cm-1 at 5.36-6.84 eV and reaches its second peak at 10.23 eV. The absorption rate then decreases with increasing energy and eventually approaches zero. Figure 8 (c) shows the loss function of SnS_2 at -5 GPa. When the energy starts to increase, the energy loss of SnS2 continues to increase, with the highest peak of energy loss at 6.51 eV. At this point, the energy loss is 3.78. As the energy continues to increase, the overall energy loss decreases, reaching 17.94 eV where the energy loss is almost zero, corresponding to the reflectance spectrum. Under negative stress of -5 GPa, the reflectivity, absorption index, refractive index, conductivity, dielectric function, and loss function all decrease to varying degrees compared to 0 GPa, with the reflectivity having the least impact and the rest decreasing by more than half of their original values.

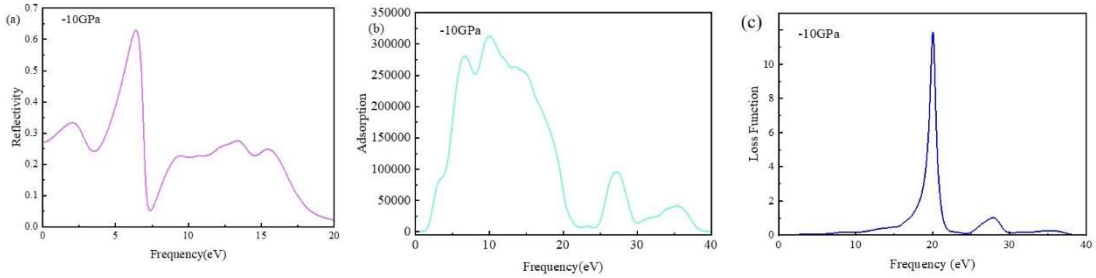

Figure 9. the optical properties of SnS_2 at -10 GPa: a) Reflectance, b) Absorption, c) Loss Function

Figure 9 (a) shows the reflectance of SnS_2 at -10 GPa. The reflectivity shows an increasing trend with the increase of energy. When the energy reaches 6.38 eV, the maximum reflectivity is 0.63. When the energy increases to 7.36 eV, the reflectivity sharply decreases to 0.049. The energy continues to increase, and the fluctuation of reflectivity finally decreases to zero. Figure 9 (b) shows the absorption rate of SnS2 at -10 GPa. According to the absorption spectrum, the absorption rate begins to increase when the energy is greater than 0.7 eV, which corresponds to the calculated band width under this stress. At an energy of 10 eV, the absorption rate reaches its maximum peak of 3.13629 × 105 cm-1. As the energy continues to increase, the absorption rate shows an overall downward trend and eventually reaches almost zero. Figure 9 (c) shows the loss function of SnS_2 at -10 GPa. From the graph, it can be analyzed that the energy loss is very small before the energy increases to 10 eV, and the maximum energy loss occurs at 20.04 eV, which is 11.92. Subsequently, the increase in energy sharply reduces the energy loss, and finally approaches zero after a slight fluctuation. Under negative stress of -10 GPa, the reflectivity, absorption index, refractive index, conductivity, dielectric function, and loss function almost all returned to the level at 0 GPa.

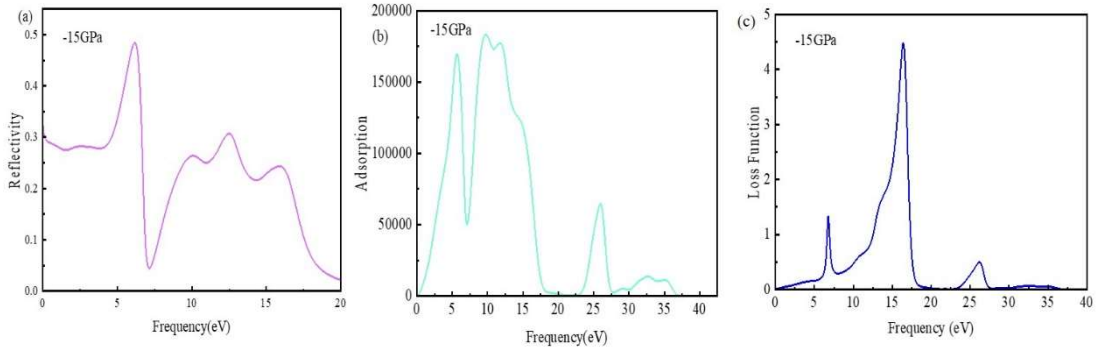

Figure 10. the optical properties of SnS_2 at -15 GPa: a) Reflectance, b) Absorption, c) Loss Function

Figure 10 (a) shows the reflectance of SnS_2 at -15 GPa. When the energy increases to 6.19 eV, the reflection peak of the reflectance reaches its maximum peak of 0.48, and then the reflectance

ISSN: 2414-1895 DOI: 10.6919/ICJE.202512_11(12).0014

decreases with the increase of energy until it finally approaches zero. Figure 10 (b) shows the absorption rate of SnS_2 at -15 GPa. The absorption rate increases with the increase of energy, reaching the first peak of 1.69917×10^5 cm^{-1} at 5.67 eV. As the energy continues to increase, the absorption rate reaches the second peak of 1.83624×10^5 cm^{-1} at 9.74 eV, which is also the maximum peak. Subsequently, the absorption rate fluctuates and decreases with the increase of energy, eventually reaching zero. Figure 10 (c) shows the loss function of SnS_2 at -15 GPa. From the graph, it can be seen that the energy loss is almost zero at two locations below 5 eV and above 20 eV. The maximum energy loss peak appears at 16.45 eV, with a maximum value of 4.47.

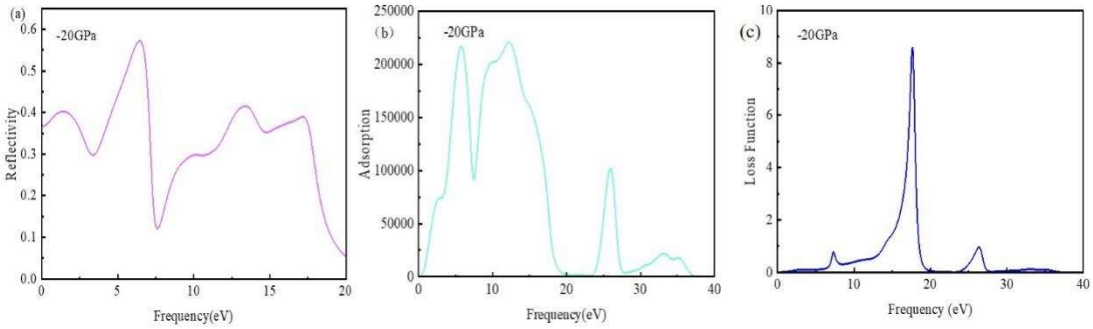

Figure 11. the optical properties of SnS_2 at -20 GPa: a) Reflectance, b) Absorption, c) Loss Function

Figure 11 (a) shows the reflectance of SnS_2 at -20 GPa. Starting from 0 eV, as the energy increases, the reflectivity increases from an initial 0.36 eV to a maximum value of 0.57 at 6.43 eV. When the energy increases to 7.60 eV, the reflectivity sharply decreases, then slowly increases to 17.16 eV and continues to decrease. Figure 11 (b) shows the absorption rate of SnS2 at -20 GPa. As the energy increases, the absorption rate increases and two peaks appear at 5.77 eV and 12.26 eV, respectively, at 2.17227×10^5 cm^{-1} and 2.21563×10^5 cm^{-1}. Finally, as the energy increases, the reflectivity decreases to zero. Figure 11 (c) shows the loss function of SnS_2 at -20 GPa. When the energy is less than 6.47 eV and greater than 20 eV, the energy loss is almost zero, with a maximum energy loss of 8.61 at 17.63 eV.

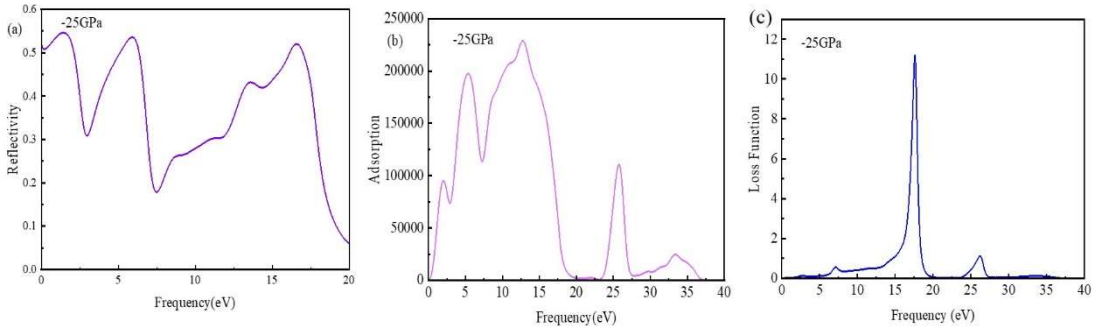

Figure 12. the optical properties of SnS_2 at -25 GPa: a) Reflectance, b) Absorption, c) Loss Function

Figure 12 (a) shows the reflectance of SnS_2 at -25 GPa. The reflectance fluctuates greatly with the increase of energy in the figure, with three different reflectance peaks appearing at 1.45 eV, 5.91 eV, and 16.58 eV, respectively. The reflectance peaks are 0.54, 0.53, and 0.52, with the maximum peak at 1.45 eV. After that, the reflectance sharply decreases with the increase of energy at 16.58 eV. Figure 12 (b) shows the absorption rate of SnS_2 at -25 GPa. The energy increased from 0 eV to 12.77 eV, and multiple absorption peaks appeared in this region. The absorption rate reached its maximum

ISSN: 2414-1895 DOI: 10.6919/ICJE.202512_11(12).0014

peak of 2.29012 × 10^5 cm^{-1} at an energy of 12.77 eV. After that, the energy continued to increase, and the absorption rate sharply decreased to 23.23 eV, then increased to a fourth peak of 1.10913 × 10^5 cm^{-1}, and then continued to decrease to zero. The absorption coefficient increases from zero, which corresponds to the calculation of no bandgap at -25 GPa. Figure 12 (c) shows the loss function of SnS_2 at -25 GPa. Before the energy increased to 6.06 eV, the energy loss was almost zero, with the maximum energy loss at 17.60 eV, reaching 11.22. Then, as the energy continued to increase, the energy loss fluctuated and decreased, ultimately reaching zero.

4. Conclusion

This article mainly calculates and analyzes the electronic structure and optical properties of SnS_2 under negative stress through first principles and molecular dynamics simulations. Research has shown that applying negative stress has a certain promoting effect on the electronic structure and optical properties of SnS_2. After systematic discussion and analysis, the following conclusions were drawn:

Before the stress decreases to -10 GPa, the valence band top and conduction band bottom of SnS_2 are located at different positions in the Brillouin zone G~L, with a bandgap value of 1.47-0.67 eV. When the stress decreases beyond -10 GPa, both the valence band top and conduction band bottom of SnS_2 are at the G point, and there is no bandgap at -25 GPa, making it a conductor. So SnS_2 belongs to indirect bandgap semiconductors in the three stages of 0 GPa, -5 GPa, and -10 GPa, and belongs to direct bandgap semiconductors in the stages of -15 GPa and -20 GPa; In both the stress free and negative stress states, SnS_2 is mainly provided by p-state electrons, with smaller contributions from other state electrons.

Starting from 0 GPa, the reflectivity of SnS_2 decreases as the stress decreases, with the highest reflectivity observed at 0 GPa; The absorption rate reaches its maximum at -10 GPa, reaching 3.13719 × 10^5 cm^{-1}. Under other stresses, the absorption rate decreases relative to 0 GPa, but all reach absorption coefficients of 100000, which can strongly absorb light energy. It is a good choice for absorption layer materials used as optoelectronic devices; The refractive index decreases with decreasing stress starting from 0 GPa, and suddenly increases to 6.11 under the action of -25 GPa; The energy loss reaches its maximum at -10 GPa and its minimum at a stress of -5 GPa.

Data Availability Statement

The data that support the findings of this study are available on request from the corresponding author.

References

[1] Mondal S, Sahoo L, Vinod C, Gautam UK. Facile transfer of excited electrons in Au/SnS2 nanosheets for efficient solar-driven selective organic transformations [J]. Applied Catalysis B: Environmental, 2021, 286: 119927.

[2] Kiruthigaa G, Manoharan C, Bououdina M, Ramalingam S, Raju C. Structure, optical and photocatalytic properties of Ce-doped SnS2 nanoflakes[J]. Solid State Sciences, 2015, 44: 32-38.

[3] Kai Dai, Jiali Lv, Jinfeng Zhang, Changhao Liag, Guangping Zhu. Band structure engineering desgin of g-C3N4/ZnS/Sns2 ternary heterojunction visible-light photocatalyst with ZnS as electron transport buffer material [J]. Journal of Alloys and Compounds, 2019, 778: 215-223.

[4] Rusu EV, Syrbu NN, Tiron AV, Zalamai VV. Band structure ans optical constants of SnS2 single crystals [J]. Materials Research Express, 2019, 6: 046203.

[5] Burton Lee-A, Tomas J.Whittles, David Hesp, Wojciech M.Linhart, Jonathan M.Skelton, Bo Hou, Richard F.Webster, Gaeme O.Dowd, Christian Reece, David Cherns, David J.Fermin, Tin D.Veal, Vin R.Dhanak, Aron Walsh. Electronic and optical properties of single crystal SnS2: an earch-abundant disulfide photocatalst [J]. Journal of Materials Chemistry A, 2016, 4: 1312-1318.

ISSN: 2414-1895 DOI: 10.6919/ICJE.202512_11(12).0014

[6] Zhao Rumeng, Wang Tianxing, Zhao Mingyu, Xia Congxin, Zhao Xu , An Yipeng, Dai Xianqi. A theoretical simulation of small-molecules sensing on an S-vacancy SnS2 monolayer[J]. Physical Chemistry Chemical Physics, 2017, 19(16): 10470-10480.

[7] Miloudi M.E.A, Liu Y, Ge Y, Ren Y, Ouadah O. First-principles calculation to investigate structural, electronic and optical properties of transition-metals intercalated bilayer SnS2[J]. Surfaces and Interfaces, 2021, 27: 101545.

[8] Zhen Qiangzhi, Wang Haiyan. Density functional study of the electronic, elastic and lattice dynamic properties of SnS2[J]. ACTA physica polonica A, 2020, 137(6): 1095-1101.

[9] Lin Wang, Xinzhe Li, Chengjie Pei, Cong Wei, Jie Dai, Xiao Huang, Hai Li. Single and few-layer 2H-SnS2 and 4H-SnS2 nanosheets for high-performance photodetection[J]. Chinese Chemical Letters, 2022, 33: 2611-2616.

[10] Zhu Bicheng, Tan Haiyan, Fan Jiajie, Cheng Bei, Yu Jiaguo, Ho Wingkei. Tuning the strength of buit-in electric field in 2D/2D g-C3N4/SnS2 and g-C3N4/ZrS2 S-scheme heterojunctions by nonmetal doping [J]. Journal of Materiomics, 2021, 7: 988-997.

[11] Chen Ying, Gui Yingang, Chen Xianping. Adsorption and gas-sensing properties of C2H4, CH4, H2, H2O on metal oxides (CuO, NiO) modified Sns2 monolayer: A DFT study[J]. Results in Physics, 2021, 28: 104680.

[12] Verma Swati, Kumar Arun, Kumar Hemant, Baghel Rahul, Goel Naveen, Verma Mohan. L. Ab-initio modelling for gas senor device: based on Y-doped SnS2 monolayer [J]. Physica E: Low-dimensional Systems and Nanostructures, 2022, 135: 114962.

[13] Li Shuankui, Liu Xuerui, Liu Yidong, Liu Fusheng, Luo Jun, Pan Feng. Optimized hetero-interface by tuning 2D SnS2 thichness in Bi2Te2.7Se0.3/SnS2 nanocomposites to enhance thermoelectric performance [J]. Nano Energy, 2017, 39: 297-305.

[14] Wang Xiaodong, Wang Jing. Effects of Pt and Au adsorption on the gas sensing performance of SnS2 monolayer: A DFT study [J]. Materials Science in Semiconductor Processing, 2021, 121: 105416.

[15] Thomas Susmi Anna, Cherusseri Jayesh. Strategically designing layered two-dimensional SnS2-based hybrid electrodes: A futuristic option for low-cost supercapacitors [J]. Journal of Energy Chemistry, 2023, 85: 394-417.

[16] Guan Yue, Li Xiaodan, Hu Taotao, Zhang Ningxia, Niu Ruixia, Liu Zhiwei. Tunable electronic properties of SnS2/WSe2 hetero-structure: A first principles study [J]. Superlattices and Microstructures, 2021, 150: 106806.

[17] Al-mamun Nahid Sultan, Wolfe Douglas.E, Haque Aman, Yim Jae Gyun, Kim Seong Keun. Room temperature annealing of SnS2 films with electron impulse force [J]. Scripta Materialia, 2023, 224: 115107.

[18] Wang Jingnan, Huang Yuhong, Ma Fei, Zhang Jianmin, Wei Xiumei, Zhu Gangqiang. Electronic states and photocatalytic performances of SnS2-based binary and ternary vdW heterostructures [J]. Journal of Alloys and Compounds, 2020, 849: 156627.

[19] Xue Yang, Zhou Wentong, Ding Lijie, Jiang Jingwen, Ning Hua, Liang Xianqing, Zhou Wenzheng, Guo Jin, Huang Dan. First-principles study on Sb-doped SnS2 as a low cost and non-toxic absorption for intermediate band solar cell [J]. Physics Letters A, 2020, 384(27): 126695.

[20] Dai Kai, Lv Jiali, Zhang Jinfeng, Liang Changhao, Zhu Guangping. Band structure engineering design of g-C3N4/ZnS/SnS2 ternary heterojunction visible-light photocatalyst with ZnS as electron transport buffer material [J]. Journal of Alloys and Compounds, 2019, 778: 215-223.

[21] He Xiancong, Shen Honglie. Ab initio calculation of band structure and thermophysical properties for SnS2 and SnSe2 [J]. Physica B: Condensed Matter, 2012, 407(7): 1146-1152.

[22] Rehman Javed, Fan Xiaofeng, Zheng W.T. Computational insight of monolayer SnS2 as anode material for potassium ion batteries [J]. Applied Surface Science, 2019, 496: 143625.

[23] Sainbileg Batjargal, Hayashi Michitoshi. Possible indirect to direct bandgap transition in SnS2 via nickel doping [J]. Chemical Physics, 2019, 522: 59-64.

[24] Saadati Amir, Sheibani Saeed. Insight into the adsorption and photocatalytic properties of in-situ synthsized g-C3N4/SnS2 nanocomposite [J]. Ceramics International, 2022, 48(20): 30294-30306.

ISSN: 2414-1895 DOI: 10.6919/ICJE.202512_11(12).0014

[25] Liu Yu, Tang Bowen, Wen Bo, Li Xibo, Zou Daifeng, Chai Yifeng, Xu Ying, Wei Xiaolin, Yin Wenjin. Non-metal atom modified SnS2 sheet for CO2 photoreduction with significant activity and selectivity improvements: A first-principles study [J]. Applied Surface Science, 2022, 584: 152618.